Enterotype identification and its influence on regulating the duodenum metabolism in chickens

Zhongyang Yuan,[a] Wei Yan,[a] Chaoliang Wen, Jiangxia Zheng, Ning Yang and Congjiao Sun[1]

National Engineering Laboratory for Animal Breeding and Key Laboratory of Animal Genetics, Breeding and Reproduction, Ministry of Agriculture and Rural Affairs, College of Animal Science and Technology, China Agricultural University, Beijing 100193, China

ABSTRACT Enterotypes are used to describe clusters of specific gut microbial community structures, but few reports exist on the identification of enterotypes in poultry. In addition, there is incomplete understanding on the role of the foregut microbiota in the digestion and absorption of nutrients in poultry. Thus, this study aimed to identify the duodenal enterotypes by examining microbial communities from 206 broilers using 16S rRNA high-throughput sequencing and explore the effects of enterotypes on phenotypic performance and nutrient metabolism with metabolomics. The duodenal microbial communities of the broiler population were partitioned into 3 enterotypes (ET1, ET2, and ET3), and significant differences were observed in α-diversity among the enterotypes ($P < 0.01$). At the genus level, the ET1 group was over-represented by *Bacteroides* (9.8%) and *Escherichia–Shigella* (8.9%), the ET2 group was over-represented by *Ochrobactrum* (19.4%) and *Rhodococcus* (14.7%), and the ET3 group was over-represented by *Bacillus* (23.4%) and *Akkermansia* (16.2%). The relative abundance of the dominant taxa of each enterotype was significantly higher than that in the other 2 enterotypes ($P < 0.01$). The results showed that *Ochrobactrum* and *Rhodococcus* were positively correlated with cellobiose, alpha-D-glucose, D-mannose, and D-allose (r = 0.429, 0.435, 0.482, and 0.562, respectively; all $P < 0.05$). *Rhodococcus* was also positively correlated with tridecanoic acid and glycerol 1-myristate (r = 0.655 and 0.489, respectively; all $P < 0.01$). In terms of phenotype, the triglyceride level in the ET2 group was significantly higher than that in the ET1 group ($P < 0.05$), and the subcutaneous fat thickness and abdominal fat weight in the ET2 group were the highest ($P > 0.05$). Taken together, these results confirmed the presence of enterotypes in broilers and found that the dominant microbes in broilers of the ET2 group might play a major role in the degradation and utilization of plant polysaccharides, which may have an impact on the serum triglyceride level and fat deposition in broilers. These findings lay a foundation for further studies on the gut microbial interactions with the metabolism in broilers and the regulation of the gut microbiota to promote growth and well-being in broilers.

Key words: enterotype, gut microbiota, metabolomics, nutrient, chicken

2020 Poultry Science 99:1515–1527
https://doi.org/10.1016/j.psj.2019.10.078

INTRODUCTION

Throughout evolution, the symbiotic relationship between a host and its gut microbiota is well documented (Bang et al., 2018). The gut microbiota is involved in the digestion of food (Ndeh et al., 2017), the absorption and metabolism of nutrients (Semova et al., 2012), and the regulation of immune function (Cervantes-Barragan et al., 2017), exerting a significant impact on the growth and well-being of the host. Recently, a number of studies have been conducted on the intestinal microbes of birds (Stanley et al., 2012; Davail et al., 2018). However, the diversity and complexity of the microbial community in the gastrointestinal tract hinders the annotation of microbial function and hence leads to a limited understanding of the interactions between the gut microbiota and the bird. The chicken is an important animal economically, and exploring the mechanism of digestion and the absorption of nutrients assisted by the gut microbiota is necessary for efficient feed utilization and animal protein production.

With the rapid development of high-throughput sequencing technology and computational methods, it has become achievable to evaluate the taxa, genes, and

Received July 20, 2019.
Accepted October 30, 2019.

[a]These authors contributed equally to this work.

[1]Corresponding author: cjsun@cau.edu.cn

genomes present in complex microbial community environments such as feces or the intestine (Ursell et al., 2012). Arumugam et al. (2011) first illustrated that there were 3 robust clusters in the human gut microbial community, referred to as enterotypes (**ET**). The ET were described as being "densely populated areas in a multidimensional space of community composition," and the differentiation between ET was mainly driven by the relative abundance of pivotal bacterial genera and not affected by sex, age, geographical location, or other factors (Arumugam et al., 2011). Since the concept of ET was proposed, a series of studies have been conducted to test their generality, with a range of 2 to 4 ET being identified in subsequent studies in humans (Koren et al., 2013; Zhou et al., 2014; Falony et al., 2016). Enterotypes have also been detected in several other animals, such as chimpanzees (Moeller et al., 2012), laboratory and wild mice (Hildebrand et al., 2013; Wang et al., 2014), and bumblebees (Li et al., 2015), proving that ET are not anthropocentric and extending their general applicability. Enterotypes provide a new perspective for understanding the differences in microbial composition and function among individuals and importantly provide a tool to search for microbial markers related to certain diseases or specific host traits. However, to the best of our knowledge, this concept is seldom used in poultry studies, and limited research has been carried out to identify ET using the gut microbiome in poultry.

Although microbiomics has been effective in aiding our understanding of the interactions between the gut microbiota and the host, a single application of microbiomics cannot directly assay the biological activity of microbes. Integration of multiple "omics" technologies will enable researchers to obtain a comprehensive understanding of the composition and function of microbial communities and provide more abundant information for the prediction and modeling of community phenotypes (Jansson and Baker, 2016). Metabolomics is a comprehensive analysis of the identification and quantification of all metabolites in biological systems (Fiehn, 2002). Association analysis between the gut metabolome and microbiome can reveal the key metabolites produced by gut microbes (Shaffer et al., 2017). Increasing attention has been paid to fecal metabolomics in humans and other animals, and this methodology shows many potential applications (Zhao et al., 2013; Zierer et al., 2018; Franzosa et al., 2019). However, there is lack of analysis of the association between microbiome and metabolome of the upper small intestine of broilers to explore the nutritional interactions between the microflora and hosts.

Therefore, the objectives of this study were as follows: (1) to identify ET using the duodenal microbial communities in 206 broilers based on a microbiomics technique and (2) to explore the effects of the different ET on the metabolism of nutrients and phenotypic performance. The findings will provide new insight into the interactions between the gut microbiota and broiler in nutrient metabolism.

MATERIALS AND METHODS

Animal Management and Sample Collection

All the experimental procedures were conducted in accordance with the guidelines for experimental animals established by the Animal Care and Use Committee of China Agricultural University (permit number: SYXK 2015–0,028).

The source of experimental animals and the process of sample collection were as previously described (Yan et al., 2019). A total of 206 meat-type male broilers from a pure line (N204) kept in Wen's Nanfang Poultry Breeding Co., Ltd. (Guangdong, China) were reared from the age of 56 to 77 D under identical conditions (including feed and water, light exposure, and immunization status). The starting body weight (**SBW**) and ending body weight (**EBW**) were recorded for all the animals. At 77 D of age, all the broilers were euthanized by cervical dislocation and dissected. Then, subcutaneous fat thickness (**SFT**) and abdominal fat weight (**AFW**) were measured, and blood was collected for the detection of serological indexes. The duodenal contents and mucosa were collected simultaneously and then mixed in a cryopreservation tube. To reduce the sampling error between individuals, a 10-cm-long fixed section of the duodenum was collected during the sampling process. All the samples were immediately placed in liquid nitrogen and stored at −80°C for extraction of 16s rRNA (n = 206) and detection of metabolites (n = 30) in the samples.

DNA Extraction and 16S rRNA Sequencing

Microbial DNA was extracted from each duodenal sample using a QIAamp DNA stool mini kit (cat # 51,504, Qiagen, Hilden, Germany) in accordance with the manufacturer's instructions. The V4 region of the bacterial 16S rRNA gene was amplified by PCR using the forward primer 520F (5′-AYTGGGYDTAAAGNG-3′) and the reverse primer 802R (5′-TACNVGGGTATC-TAATCC-3′). Sample-specific 7-bp barcodes were incorporated into the primers for multiplex sequencing. The PCR reaction mixtures contained 5 μL of 5 × Q5 reaction buffer, 5 μL of 5 × Q5 High-Fidelity GC buffer (Qiagen), 2 μL of DNA template, 1 μL (10 μM) of each forward and reverse primer, 2 μL of dNTPs (2.5 mM), 0.25 μL of Q5 High-Fidelity DNA polymerase (Qiagen) (5 U/μL), and 8.75 μL of ddH_2O. The PCR conditions were as follows: 98°C for 2 min, followed by 25 cycles at 98°C for 15 s, 55°C for 30 s, and 72°C for 30 s, and a final extension at 72°C for 5 min. All PCR products were purified using Agencourt AMPure Beads (Beckman Coulter, Indianapolis, IN) and quantified using a PicoGreen dsDNA assay kit (Invitrogen, Carlsbad, CA). After quantification, PCR amplicons were pooled in equal amounts and sequenced using the paired-end approach on the Illumina MiSeq platform using the MiSeq Reagent kit version 3 at Shanghai Personal Biotechnology Co., Ltd. (Shanghai, China).

Bioinformatics Analysis

Sequencing data analysis was performed using the Quantitative Insights Into Microbial Ecology 2 (**QIIME2**, version 2018.6, https://docs.qiime2.org/2018.6) microbiome data science analysis platform. First, the QIIME2 quality-filter q-score and deblur denoise-16S plug-ins were used to perform raw data quality control, including filtration of low-quality and noisy sequences, removal of chimeras, and dereplication. Different from the previous method of clustering based on sequence similarity, QIIME2 generates a clustering feature table using a dereplication approach, which contains all the unique sequences observed in the data set. The feature table is equivalent to the table showing operational taxonomic units (**OTU**) with 100% similarity, which is more accurate than the analysis results of the previous generation. Then, the QIIME2 feature-table filter-features plug-in was used to filter the obtained features. In our study, only those features that accounted for more than 0.001% of the total frequency in all individuals and appeared in at least 3 individuals were used to improve the efficiency of further analysis.

Based on the obtained effective feature sequences, we used QIIME2 and the Naive Bayes classifiers trained on Silva 132 99% OTUs from the 515F/806R region of the sequences (https://data.qiime2.org/2018.6/common/silva-132-99-515-806-nbclassifier.qza) to perform taxonomy classification. The Quantitative Insights Into Microbial Ecology 2 taxa barplot plug-in was used to visualize the microbial composition of samples at different levels. Quantitative Insights Into Microbial Ecology 2 taxa collapse and feature-table relative-frequency plug-ins were used to calculate the relative abundance of samples at specified taxonomic levels.

Enterotype Clustering and Functional Prediction of Dominant Bacterial Genera

Enterotype analysis was implemented as previously described (Arumugam et al., 2011; Koren et al., 2013). We adopted the PAM clustering algorithm in the R package "cluster" to identify ET at the genus taxonomic level and applied the 2 diversity metrics, namely, the Jensen–Shannon divergence (**JSD**) and the Bray–Curtis (**BC**) similarity index, to calculate distance. The prediction strength (**PS**) and silhouette index (**SI**) of clusters were used to determine the optimal number of clusters, and these 2 indexes were considered absolute measures of cluster quality in this study. Principal coordinate analysis was performed via the dudi.pco function in the R package "ade4."

For α-diversity analysis, the QIIME2 diversity plug-in was used to calculate the observed species and the Shannon index at a sampling depth of 3,500, and then a nonparametric statistical method (Kruskal–Wallis test) was used to compare the diversities among ET. A P-value of less than 0.05 was considered statistically significant. To compare the microbial composition among ET, the dominant microbial taxa were statistically analyzed at the phylum and genus levels, and the Kruskal–Wallis test was used to compare the relative abundance of microbial taxa. A P-value of less than 0.05 was considered statistically significant.

Phylogenetic Investigation of Communities by Reconstruction of Unobserved States (**PICRUSt**, http://galaxy.morganlangille.com/), version 1.1.1, was used to predict the functional profile of all dominant bacterial genera identified from 3 ET based on the 16S rRNA gene sequences obtained. The "Normalize by Copy Number" command was performed to correct the OTU table for multiple 16S copy numbers, and the metagenomes were predicted using precalculated Kyoto Encyclopedia of Genes and Genome (**KEGG**) orthologs for each sample in the given OTU table. The predicted metagenomes were collapsed into the KEGG pathway hierarchy level 3 using the KEGG pathway metadata. The main pathways were analyzed as per ET, and the Kruskal–Wallis test was used to compare the enriched sequences of the pathway. A P-value less than 0.05 was considered statistically significant.

Individual Selection and Phenotypic Data Analysis

After ET clustering, the first 3 dominant genera in each ET were extracted. The SI score can be used as a criterion to evaluate the robustness of an individual belonging to one ET. To explore the effects of ET on the metabolism of nutrients and phenotypic performance, based on the SI value obtained from the BC distance partition and the relative abundance of dominant genera, 10 representative samples from each ET were selected as subpopulations for metabolomics detection and phenotype analysis. The specific selection criteria were as follows: the SI value ranked in the top 15 (ET2 ranked in the top 30) and the relative abundance of the dominant genera were higher than the average within the group. Then, the relative abundance of the dominant bacterial genera in a subpopulation was statistically analyzed.

The broiler phenotypes of 3 subpopulations were analyzed, including the SBW, EBW, SFT, and AFW. In addition, the serum low-density lipoprotein cholesterol (**LDL-C**), high-density lipoprotein cholesterol, and triglyceride (**TG**) levels were measured and analyzed. The ANOVA test was used to compare the phenotypic data, and a P-value less than 0.05 was considered statistically significant.

Metabolomics Profiling by Ultrahigh Performance Liquid Chromatography–Tandem Mass Spectrometry

The ultrahigh performance liquid chromatography–tandem mass spectrometry (**UHPLC–MS/MS**) method was used for untargeted metabolomics analysis in consideration of its high efficiency, sensitivity, and peak resolution. To facilitate analysis, 30 selected

samples were preprocessed as per the following protocol. First, 0.2 mL of ultrapure water was added to each sample of duodenal contents (60 ± 0.1 mg), and the suspension was fully homogenized in a bead mill. Then, 0.8 mL of methanol–acetonitrile mixture (v/v, 1:1) was added to each sample, and after mixing with a vortex mixer, all samples were broken by ultrasonic waves at low temperature. Next, the samples were incubated to precipitate the protein at −20°C for 1 h. After centrifugation at 13,000 rpm at 4°C for 15 min, 0.5 mL of the supernatant was collected and freeze-dried for storage.

The LC separation was performed using an Agilent 1290 Infinity LC UHPLC System and an HILIC chromatographic column (Agilent, Waldbronn, Germany), at a temperature of 25°C, a flow rate of 0.3 mL/min, and a sample size of 2 μL. The mobile phase consists of phase A (H_2O +25 mM NH_4Ac + 25 mM $NH_3 \cdot H_2O$) and phase B (CH_3CN). The gradient elution procedure for the mobile phase change was as follows: 0 to 1 min, 95% B; 1 to 14 min, with B changing from 95% linear to 65%; 14 to 16 min, with B changing from 65% linear to 40%; 16 to 18 min, with B being maintained at 40% for 2 min; 18 to 18.1 min, with B changing from 40% linear to 95%; and 18.1 to 23 min, with B being maintained at 95%. The samples were placed in a 4°C automatic sampler, with the A phase and the B phase totaling 100% during the whole analysis process. To avoid the influence of fluctuations in the signal detected by the instrument, a random order was used for continuous analysis of the samples.

After separating the samples by UHPLC, a triple time of flight (**TOF**) 5600 mass spectrometer (AB SCIEX, Redwood, CA) was used for mass spectrometry analysis. Electrospray ionization patterns of positive and negative ions were used for further detection. Electrospray ionization source-dependent conditions were set as follows: ion source gas 1: 60, ion source gas 2: 60, and curtain gas: 30, source temperature: 600°C, IonSpray Voltage Floating: ± 5,500 V (2 modes of positive and negative ions), TOF MS scan m/z range: 60 to 1,000 Da, product ion scan m/z range: 25 to 1,000 Da, TOF MS scan accumulation time: 0.20 s/spectra, and product ion scan accumulation time: 0.05 s/spectra. Information-dependent acquisition was used to obtain the second-order mass spectra, and a high sensitivity model was adopted.

Metabolomics Data Analysis and Association Analysis

To facilitate the association analysis of the microbiome data, including format conversion, peak alignment, retention time correction, and peak area extraction, the metabolome raw data were preprocessed using ProteoWizard (Kessner et al., 2008) and XCMS (Tautenhahn et al., 2012) tools. The metabolite structure was identified by means of accurate mass number matching (<25 ppm) and second-order spectrogram matching. SIMCA-P 14.1 (Umetrics, Umea, Sweden) was used for pattern recognition. After the data were preprocessed by Pareto scaling, one-way statistical analysis, including the Mann–Whitney U test and fold change (**FC**) analysis, was performed between the subpopulations. Significantly altered metabolites were identified as per the following criteria: *P*-values less than 0.05 in the Mann–Whitney U test and FC > 2.0 or <0.5 in FC analysis. Spearman correlation coefficients were used to identify the correlations between microbes and metabolites with significant differences among subpopulations. Graphing and statistical analyses were conducted using the GraphPad Prism program (version 6.0, GraphPad Software Inc., La Jolla, CA) and SPSS software (version 20.0, IBM, Armonk, NY).

RESULTS

Microbial Community Composition and the Detection of ET

A total of 6,684 features and 1,623,319 sequences were obtained from 206 individuals after quality control, and these valid sequences were annotated to represent 31 phyla and 679 genera by taxonomy classification. At the phylum level, the 4 most abundant phyla that accounted for 90% of the population included Proteobacteria (34.74%), Firmicutes (24.38%), Bacteroidetes (15.31%), and Actinobacteria (15.07%) (Supplementary Figure 1A). At the genus level, more than 98% of sequences were annotated, and the dominant genera were *Ochrobactrum* (14.60%), *Rhodococcus* (12.26%), *Bacillus* (9.14%), and *Vibrionimonas* (5.29%) (Supplementary Figure 1B).

Enterotype analysis revealed that broiler population could be divided into 3 distinct ET based on BC and JSD distances (Figure 1) because the maximum PS values and SI scores were obtained when there were 3 clusters (Supplementary Figure 2). Although the results of ET identification using 2 distances showed slight differences in the number of samples in each of the corresponding groups, there were still more than 87.5% of individuals within the same ET on average (Supplementary Figure 3), indicating that both of these distances could classify the ET of the population effectively and had no significant effect on the grouping. Because the BC distance had a significantly higher average SI value than the JSD distance (BC vs. JSD, 0.276 ± 0.108 vs. 0.214 ± 0.104, $P < 0.001$), our subsequent analysis was based on the 3 ET identified with the BC distance metric.

Microbiota Structures and Functional Predictions of the Different ET

For α-diversity, the observed species index was used to evaluate the community richness of each ET, and the Shannon index was used to evaluate the microbiota diversity. These 2 indexes in the ET1 and ET2 groups were significantly higher than in the ET3 group (Supplementary Figure 4), indicating that the microbial

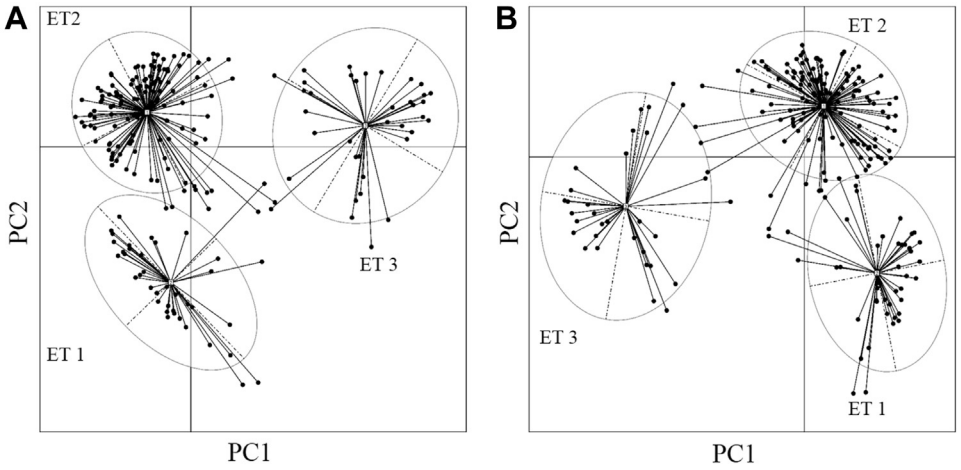

Figure 1. Principal coordinate analysis (PCoA) plot of enterotype clusters observed in the broiler population (n = 206). Three enterotypes were present when (A) Bray–Curtis distance metric and (B) Jensen–Shannon divergence distance metric were used, respectively, with each black dot representing one sample and the ellipse region representing a high sample density. Abbreviation: ET, enterotype.

diversity in the ET3 group was the lowest, and the standard deviation of the ET3 group was the lowest, indicating the microbial similarity among these samples is higher.

The microbiota taxonomic distributions of the three ET at the phylum and genus levels were analyzed and visualized (Supplementary Figure 5). The microbial composition of the ET1 and ET2 groups was similar at the phylum level, with the dominant phyla in each ET accounting for more than 90% of the population (Supplementary Table 1). Proteobacteria, Firmicutes, and Actinomycetes were the dominant microbes in the ET1 and ET2 groups, and their relative abundance was significantly higher than that in the ET3 group ($P < 0.001$). The relative abundance of the dominant phyla Firmicutes and Verrucomicrobia in the ET3 group was significantly higher than that in the other 2 ET ($P < 0.001$). At the genus level, the species and relative abundance of the dominant microbes were different among ET (Supplementary Table 2). *Bacteroides* and *Escherichia–Shigella* were the dominant genera in the ET1 group, accounting for 9.8 and 8.9% of the population, respectively; *Ochrobactrum* and *Rhodococcus* were the dominant genera in the ET2 group, accounting for 19.4 and 14.7% of the population, respectively; and *Bacillus* and *Akkermansia* were the dominant genera in the ET3 group, accounting for 23.4 and 16.2% of the population, respectively. The relative abundance of the dominant bacterial genera in each ET was significantly higher than that in the other 2 ET ($P < 0.01$).

To compare the functions of the gut microbiota among different ET, the KEGG pathway was predicted by PICRUSt. The accuracy of this prediction was assessed by the nearest sequenced taxon index values, with smaller values indicating higher accuracy. In the present study, the average nearest sequenced taxon index values for the ET1, ET2, and ET3 groups were 0.058 (±0.016), 0.087 (±0.027), and 0.037 (±0.014), respectively. PICRUSt functional inferences revealed several KEGG pathways differed significantly among ET (Supplementary Table 3). Genes related to "butanoate metabolism," "propanoate metabolism," "fatty acid metabolism," "valine, leucine, and isoleucine degradation," and "tryptophan metabolism" were predicted at significantly higher levels in the ET2 group. Genes related to "ribosome," "peptidases," "chromosome," "pyrimidine metabolism," and "amino acid–related enzymes" were predicted at significantly higher levels in the ET3 group, and no significantly increased pathways were found in the ET1 group.

Individual Selection and Phenotypic Data Analysis

As per the preset selection criteria, 10 samples were selected as subpopulations from the ET1, ET2, and ET3 groups, with SI values of 0.405, 0.370, and 0.411, respectively, the values being higher than those of the basic groups of each ET (0.289, 0.275, and 0.264, respectively, $P < 0.01$). Notably, although the selection of samples was based on the SI values obtained by ET partitioning with BC distance, these 30 samples were also stable in the 3 corresponding ET obtained by the JSD distance metric. In addition, the relative abundance of the dominant microorganisms identified previously at the genus level was statistically analyzed for further association analysis with the metabolome data (Figure 2), and the relative abundance of the dominant genera in each subpopulation was significantly higher than that for the other 2 subpopulations.

The phenotypic data for broiler chickens selected from each ET were analyzed (Table 1). We found that the average SBW in the ET3 group was the highest at 1,606.11 g and was the lowest at 1,561.50 g in the ET2 group, and there was no significant difference among the 3 ET groups ($P > 0.05$). The EBW was the highest in the ET3 group, while the results of the ET1 and ET2 groups showed an opposite trend to that of SBW, although there was no significant difference in

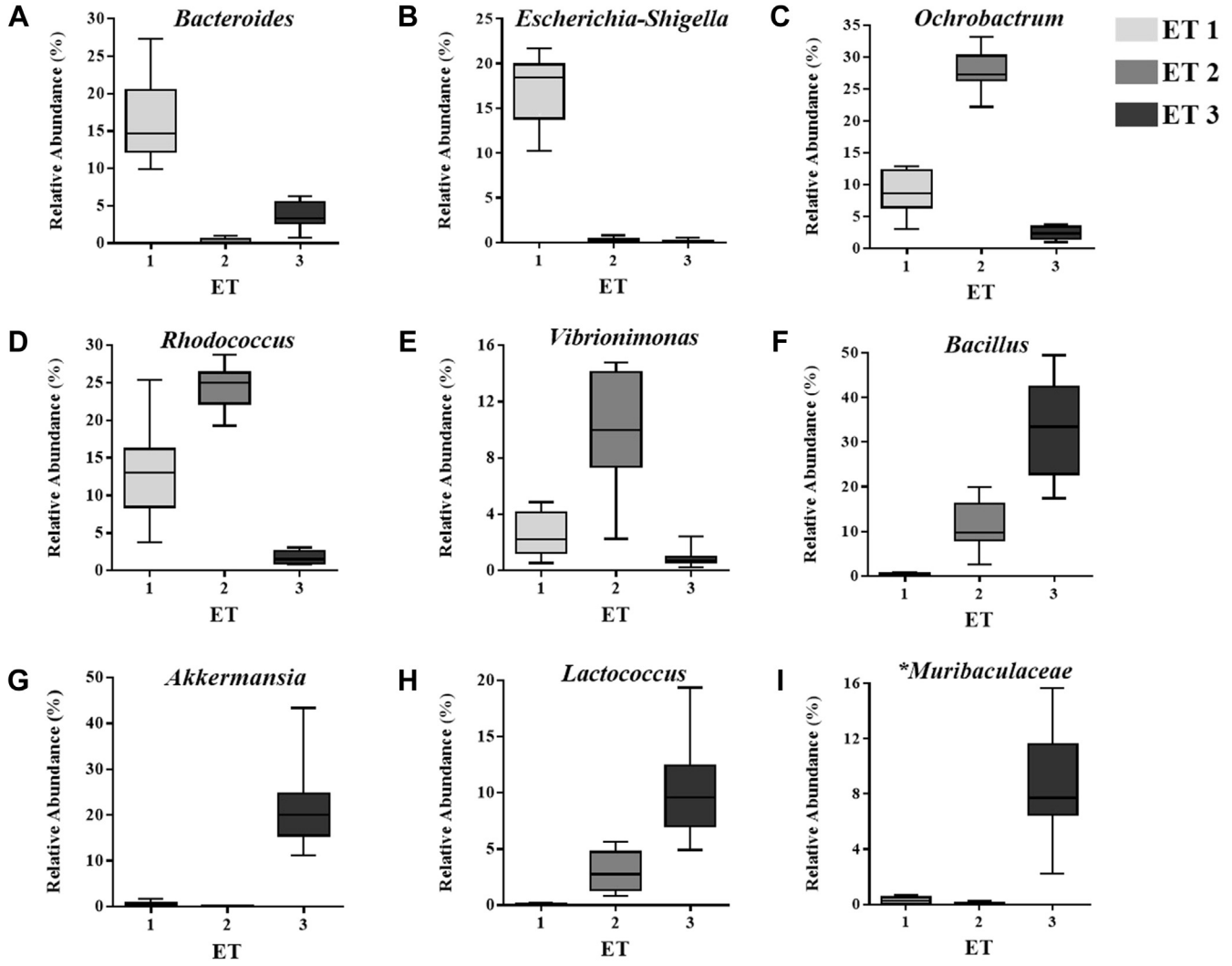

Figure 2. The boxplots show relative abundance of the over-represented bacterial genera in each subpopulation (n = 30). Unidentified genera were asterisked (*) at the name of the family level. The boxplot shown are means, ranges, and the first and third quartiles. Abbreviation: ET, enterotype.

the results ($P > 0.05$). There was no significant difference in the SFT and AFW values among the 3 ET groups ($P > 0.05$), but the maximum values were observed in the ET2 group (0.235 mm and 49.87 g, respectively). It should be noted that the ET2 group did not have the largest EBW. The results of the serological indexes showed that there was no significant difference in the content of low-density lipoprotein cholesterol and high-density lipoprotein cholesterol among the 3 ET groups ($P > 0.05$), whereas the TG content in the ET2 group was 0.352 mmol/L, which was significantly higher than 0.278 mmol/L in the ET1 group ($P < 0.05$), and showed no significant difference compared with that in the ET3 group ($P > 0.05$). These results were consistent with the patterns of the AFW and SFT results.

Detection of Metabolites and Correlation Analysis With Microbes

Because most metabolites in the sample are unknown and the signal induction intensity of the metabolites is different in the positive and negative ion modes, we used 2 ion mode–switching scanning

Table 1. Phenotypic data of selected broilers for metabolomics from three enterotypes[1].

ET	SBW (g)	EBW (g)	SFT (mm)	AFW (g)	LDL-C (mmol/L)	HDL-C (mmol/L)	TG (mmol/L)
ET1	1,598.60 ± 142.77	2,274.95 ± 333.04	0.215 ± 0.061	44.46 ± 19.38	0.993 ± 0.250	2.550 ± 0.304	0.278 ± 0.060[b]
ET2	1,561.50 ± 141.32	2,2358.00 ± 325.30	0.235 ± 0.042	49.87 ± 22.76	1.009 ± 0.474	2.331 ± 0.303	0.352 ± 0.052[a]
ET3	1,606.11 ± 118.95	2,382.33 ± 218.68	0.219 ± 0.060	43.36 ± 15.33	0.981 ± 0.349	2.454 ± 0.353	0.332 ± 0.084[a,b]

[a,b]Different superscripts within a column indicate significant difference ($P \leq 0.05$).

Abbreviations: AFW, abdominal fat weight; EBW, ending body weight; ET, enterotype; HDL-C, high-density lipoprotein cholesterol; LDL-C, low-density lipoprotein cholesterol; SBW, starting body weight; SFT, subcutaneous fat thickness.

[1]Data are presented as means ± standard deviation (SD) (n = 10 per enterotype).

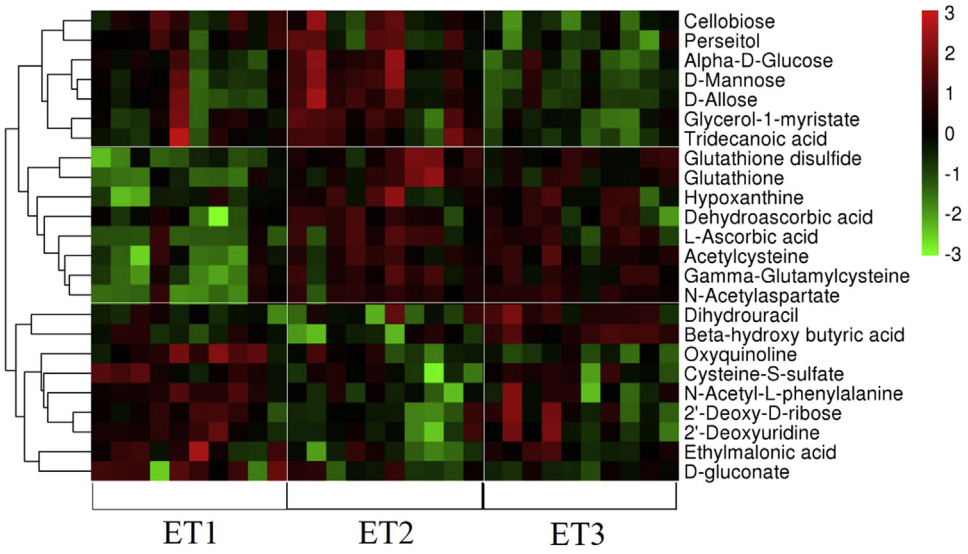

Figure 3. The heat map shows small-molecule metabolites with significant differences in relative abundance between enterotypes (n = 30). Rows represent the 24 altered metabolites, and columns represent the 30 samples selected with typical microbial community structures from each enterotype. Each column represents a sample, with the first 10 columns, the second 10 columns, and the last columns representing the ET1, ET2, and ET3 subpopulation, respectively. Abbreviation: ET, enterotype.

methods for detection. A total of 24 significantly altered metabolites were found, including 8 metabolites in the positive ion mode, 13 metabolites in the negative ion mode, and 3 metabolites in both modes (Supplementary Table 4). These metabolites showing significant differences were clustered into 3 groups as per the ET (Figure 3). Seven metabolites were upregulated in the ET2 group, including 5 sugars and 2 long-chain fatty acids (**LCFA**); 8 metabolites were downregulated in the ET1 group, mainly including glutathione and its derivatives; and another 9 different substances were clustered into one group and upregulated in the ET1 group.

We found that each subpopulation had a distinct set of bacterial genera, and metabolomic analysis revealed that microbial differences had an impact on metabolic profiling in the intestinal tract. We further explored the functional correlations between the key bacterial genera and the altered metabolites through correlation analysis based on Spearman's correlation coefficient (Table 2). Strong correlations between several specific bacterial genera and typical metabolites were revealed through this association analysis. Among them, the over-represented *Ochrobactrum* in the ET2 group was positively correlated with 4 sugars, including cellobiose ($r = 0.429$, $P = 0.0181$), α-D-glucose ($r = 0.435$, $P = 0.0163$), D-allose ($r = 0.482$, $P = 0.0070$), and D-mannose ($r = 0.562$, $P = 0.0013$) (Figure 4); *Rhodococcus* was also positively correlated with cellobiose ($r = 0.469$, $P = 0.0021$) and alpha-D-glucose ($r = 0.546$, $P = 0.0019$) (Figures 5A, 5B), whereas these 2 bacterial genera were negatively correlated with beta-hydroxybutyric acid (all $P < 0.01$). At the same time, *Rhodococcus* was significant positively correlated with 2 LCFA, namely, tridecanoic acid ($r = 0.655$, $P = 0.0003$) and glycerol 1-myristate ($r = 0.489$, $P = 0.0044$) (Figures 5C, 5D).

DISCUSSION

As an effective analytical method, population stratification can offer insight into complex biological problems relating to human health and well-being (Costea et al., 2018). When this method was applied to the study of the gut microbiota, it aided our understanding of the variation within microbial community structures. In the present study, 3 ET were identified in broiler populations based on the duodenal microbial community, which further proved the existence of ET in poultry.

Arumugam et al. (2011) used the Calinski–Harabasz index as the main standard for ET clustering, coupled with the SI to assess the robustness of ET, although the SI value was low. The practicality and relative stability of these 2 indicators has been proven in other studies (Moeller et al., 2012; Zhou et al., 2014), but some research studies have also shown that using different clustering methods, distance metrics and OTU classification levels ultimately result in different ET numbers (Koren et al., 2013; Costea et al., 2018). In our study, based on the PS scores, the broiler population could be partitioned into 3 moderate support clusters with the highest scores of 0.81 and 0.85 corresponding to the JSD and BC distance metrics, and these scores were higher than those reported in a previous study of the human gut microbiome that used the same distance metrics (Koren et al., 2013). The SI values of >0.5 and ≥ 0.75 were used as thresholds for moderate clustering and strong clustering, respectively, in previous studies (Wu et al., 2011; Koren et al., 2013), but the SI values showed a large range (0.2–0.65) across different studies (Wu et al., 2011; Qin et al., 2012; Yatsunenko et al., 2012; Mach et al., 2015). In our study, although both the distance metrics methods showed a maximum SI score when the clustering number was 3, the threshold

Table 2. Spearman's correlation coefficients between unique bacterial genera and altered metabolites in the subpopulations (n = 30).

	Bacterial genera								
Altered metabolites	*Bacteroides*	*Escherichia–Shigella*	*Ochrobactrum*	*Rhodococcus*	*Vibrionimonas*	*Bacillus*	*Akkermansia*	*Lactococcus*	[1]*Muribaculaceae*
Dihydrouracil	−0.009	−0.312	−0.339	−0.506	−0.274	0.377	0.342	0.452	0.553
Beta-hydroxybutyric acid	0.138	−0.247	−0.546	−0.640	−0.604	0.453	0.629	0.413	0.565
Oxyquinoline	0.354	0.442	0.120	0.222	0.106	−0.496	−0.182	−0.498	−0.236
2-Dehydro-3-deoxy-D-gluconate	0.363	0.223	−0.041	0.095	0.004	−0.335	−0.045	−0.237	−0.022
Ethylmalonic acid	0.418	0.163	−0.393	−0.369	−0.396	0.004	0.301	0.072	0.242
N-Acetyl-L-phenylalanine	0.557	0.307	−0.280	−0.127	−0.152	−0.412	0.147	−0.375	0.161
2′-Deoxy-D-ribose	0.469	0.085	−0.341	−0.332	−0.268	−0.200	0.271	−0.158	0.327
Cysteine-S-sulfate	0.422	0.257	−0.279	−0.152	−0.344	−0.240	0.119	−0.235	0.263
2′-Deoxyuridine	0.516	0.215	−0.257	−0.240	−0.209	−0.317	0.117	−0.259	0.234
Acetylcysteine	−0.585	−0.474	0.040	−0.044	0.011	0.475	−0.074	0.494	−0.045
N-Acetylaspartate	−0.534	−0.466	0.099	0.011	0.140	0.381	−0.074	0.369	−0.015
gamma-Glutamylcysteine	−0.615	−0.441	0.202	0.075	0.195	0.381	−0.080	0.411	−0.055
L-Ascorbic acid	−0.600	−0.412	0.154	0.022	0.161	0.434	−0.161	0.421	−0.096
Glutathione disulfide	−0.645	−0.650	0.232	0.120	0.186	0.506	−0.114	0.521	0.053
Glutathione	−0.656	−0.506	0.313	0.204	0.238	0.336	−0.155	0.342	−0.151
Hypoxanthine	−0.366	−0.427	−0.053	0.055	−0.005	0.412	0.020	0.428	0.245
Dehydroascorbic acid	−0.462	−0.200	0.145	0.221	0.251	0.190	−0.199	0.246	−0.115
Glycerol 1-myristate	−0.242	0.054	0.340	0.489	0.380	−0.229	−0.524	−0.212	−0.432
Cellobiose	−0.098	0.206	0.429	0.469	0.355	−0.329	−0.494	−0.320	−0.532
Perseitol	−0.072	0.236	0.309	0.451	0.264	−0.286	−0.439	−0.300	−0.426
D-Allose	−0.473	−0.088	0.482	0.551	0.556	−0.095	−0.560	−0.011	−0.490
Tridecanoic acid	−0.268	0.065	0.487	0.655	0.515	−0.338	−0.598	−0.320	−0.535
D-Mannose	−0.400	0.070	0.561	0.626	0.528	−0.209	−0.660	−0.146	−0.585
α-D-Glucose	−0.295	0.120	0.435	0.546	0.500	−0.189	−0.596	−0.139	−0.507

[1]Unidentified genera were asterisked at the name of the family level.

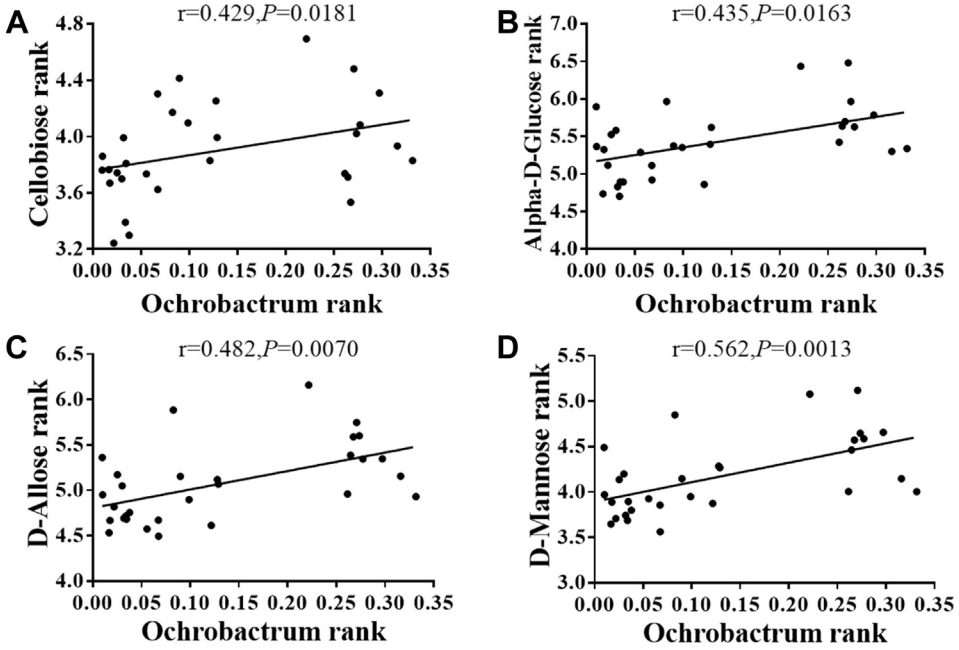

Figure 4. The scatter plots with correlation coefficients show the high correlation between the key bacterial genus *Ochrobactrum* and metabolites of (A) cellobiose, (B) alpha-D-glucose, (C) D-allose, and (D) D-mannose, respectively (n = 30). The horizontal axis represents the raw relative abundance of bacteria, and the vertical axis is $\log_{10}$-transformed from the raw measurements (normalized) of metabolites. The given r values indicate Spearman's rank correlation, and the *P* value represents the significance of the test result.

for moderate clustering (SI > 0.5) was not reached. Regarding the criteria for judging the number of ET, we believe that more experimental data are needed to determine a more reasonable SI score threshold. Unlike a previous study that divided the broiler population into 4 ET (Kaakoush et al., 2014), we detected 3 ET in this study. This may be because we used data from the gut microbiome in the duodenum, whereas the previous study used data from the fecal microbial community, and some studies have shown that the microbial community structure of the 2 sites is different (Choi et al., 2014; Xiao et al., 2017).

The results of microbial diversity analysis showed that the number of observed species and the Shannon index were lowest in the ET3 group, indicating that the ET3 group has the lowest microbial richness and evenness.

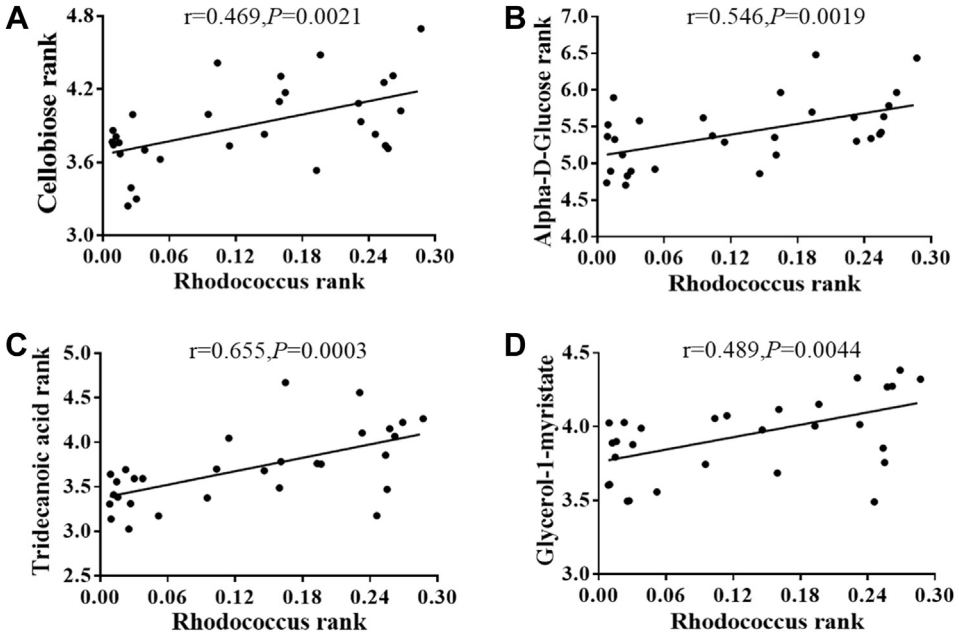

Figure 5. The scatter plots with correlation coefficients show the high correlations between the key bacterial genus *Rhodococcus* and metabolites of (A) cellobiose, (B) alpha-D-glucose, (C) tridecanoic acid, and (D) glycerol 1-myristate, respectively (n = 30). The horizontal axis represents the raw relative abundance of bacteria, and the vertical axis is $\log_{10}$-transformed from the raw measurements (normalized) of metabolites. The given r values indicate Spearman's rank correlation, and the *P* value represents the significance of the test result.

In addition, it should be noted that the relative abundance of Firmicutes as the dominant phylum in the ET3 group was high, which is consistent with previous reports (Huse et al., 2012; Zupancic et al., 2012). The high relative abundance of Firmicutes in the ET3 group may have an inhibitory effect on other microbes, resulting in the decrease in gut microbial diversity in the ET3 group. As previously reported in human and other animal studies (Arumugam et al., 2011; Wang et al., 2014; Liang et al., 2017), *Bacteroides* was the dominant microbial genus over-represented in the broilers of the ET1 group. We also identified *Escherichia–Shigella* as another driving genus in the ET1 group, a genus previously detected in the ET2 group of broilers (Kaakoush et al., 2014). The ET2 group was over-represented by *Ochrobactrum* and *Rhodococcus*, and over-representation of these genera had not previously been reported in any ET. *Bacillus* and *Akkermansia* were over-represented in the ET3 group of broilers, and *Akkermansia* was also over-represented in human ET3. In addition, the ET3 group was dominated by Firmicutes, accounting for nearly 50% of the population at the phylum level, and it has an abundance advantage compared with the other phyla, which may be the main reason why microbial diversity in the ET3 group was lower than that in the ET1 and ET2 groups.

It has been proven that the differences in the microbial community structure that result in functional and ecological properties are different among ET (Costea et al., 2018). Previous studies reported that the *Bacteroides* and *Prevotella* ET had different characteristics in terms of digestive function. The former is prone to occur in populations with high-animal-fat and protein diets, and meat consumption in Western diets is characteristic of this ET, whereas the latter is more readily found in individuals on diets high in plant carbohydrates, where high ratios of simple sugars are present (De Filippo et al., 2010; Wu et al., 2011). In the present study, significant differences in functional changes among ET were observed, indicating that this difference in ecological properties also existed in broiler ET. For example, broiler ET2 was enriched in 'fatty acid metabolism'– and 'propanoate metabolism'–related genes, suggesting that it was more closely associated with energy metabolism. We believe that this difference in population function caused by different microbial community structures will produce different results in the interactions between bacteria and broilers, thereby affecting the health and growth of broilers themselves.

To explore the effects of microbial community structure differences among ET on the metabolism of nutrients and phenotypic performance, we performed an in-depth analysis and metabolic profiling of the subpopulations of each ET. Through metabolomic analysis, we found that there was a significant excess of simple sugars present in the ET2 group, suggesting that it may have the same biological characteristics as the *Prevotella*-dominated ET2 previously found in mammals. Correlation analysis between distinct bacterial genera and altered metabolites identified in each subpopulation revealed high correlations between *Ochrobactrum* and *Rhodococcus*, with several small molecule metabolites. Because the functional prediction results showed that sequences enriched in some metabolic pathways of these 2 microbes were more significant, we focused on these 2 bacterial genera. *Ochrobactrum* and *Rhodococcus* showed a significant positive correlation with simple sugars such as cellobiose, α-D-glucose, D-allose, and D-mannose, and we therefore hypothesize that these genera possess the physiological characteristics of degrading and extracting energy from plant polysaccharides. *Ochrobactrum* belongs to a genus of the Rhizobiaceae family, and its members include some rhizobial species. It has been reported for the first time that strain DASA 35030 of *Ochrobactrum* was able to establish a symbiotic nitrogen-fixing relationship with a host plant (Ngom et al., 2004), and in later studies, it has been reported that some other strains belonging to *Ochrobactrum* were shown to establish symbiotic relationships with their host plants (Zurdo-Pineiro et al., 2007; Imran et al., 2010; Woo et al., 2011). Rhizobial symbioses with leguminous plants and a few nonleguminous plants result in the formation of nodules, which can reduce molecular nitrogen in the air to available nitrogen to plants, thereby playing an important role in the nitrogen cycle in nature (Franche et al., 2009). One of the reasons why rhizobia can nodulate with the host is that they secrete cellulase and hemicellulose that degrade the cell wall of root hairs, thus allowing infection through this point of entry (Cocking, 2003). In this study, excessive levels of cellobiose were detected in the ET2 group, which comprises the simple structure of cellulose and glucose monomers, while allose and mannose are the simple sugar structures of hemicellulose. It is well known that broilers cannot digest and use complex polysaccharides such as cellulose and hemicellulose, and gut microbes play a key role in degrading these substances (Cho et al., 2012). In rhizobia, the over-representation of *Ochrobactrum* in the ET2 group probably plays a role in the biodegradation of plant fibers to generate simple sugars such as cellobiose and mannose, which will be further metabolized and used as a source of energy for broilers and bacteria.

Unlike *Ochrobactrum*, *Rhodococcus* does not degrade cellulose, but studies have shown that it can mediate the degradation of lignin and its derivatives, and it can use the biphenyl moieties introduced by lignin decomposition as carbon-rich resources (Kosa and Ragauskas, 2012). Lignin is a phenolic heteropolymer with a heterogeneous structure, which together with cellulose and hemicellulose forms the main structure of the plant cell wall (Plomion et al., 2001). In this study, we observed a positive correlation of *Rhodococcus* with cellobiose and α-D-glucose, and this might indicate that *Rhodococcus* can accelerate the degradation of cellulose by *Ochrobactrum* during the process of lignin degradation. In addition, *Rhodococcus* also showed a positive correlation with 2 LCFA, namely, tridecanoic acid and glycerol 1-myristate. The results of functional prediction showed

that the number of fatty acid metabolism pathways in *Rhodococcus* was significantly higher than for other microbes. In addition to the functional property of lignin degradation mentioned previously, another common feature of *Rhodococcus* is the accumulation of triacylglycerols (Alvarez et al., 2000; MacEachran et al., 2010), which can use a variety of fermentation substrates including lignin as carbon sources to generate lipids, and the efficiency of lipid synthesis varies among different *Rhodococcus* strains. The production of lipids in these microbes involves 3 steps: (1) the production of fatty acyl compounds, (2) the formation of glycerol intermediates, and (3) the sequential esterification of glycerol moieties with fatty acyl residues (Liu et al., 2018). In our study, the significant positive correlation between *Rhodococcus* and 2 LCFA proved that it can synthesize lipids, although based on our current method, it is unclear which specific bacterial species or strains produce lipid.

The renewable lignocellulosic biomass that exists in plants is an organic polymer that is ubiquitous in nature; however, its biotransformation and utilization have always been a challenge because to its recalcitrant nature. Some bacteria can naturally degrade plant cellulose for fermentation and utilization, and there has been a research effort to identify such microbes in recent years (de Gonzalo et al., 2016; Wilhelm et al., 2019). Our study showed that the dominant microbes in broiler ET2, *Ochrobactrum* and *Rhodococcus*, can perform combined degradation of lignocellulose biomass, namely, the saccharification of lignocellulose. This process involves 2 steps: (1) the production of simple sugars from combined degradation by *Ochrobactrum* and *Rhodococcus* and (2) the synthesis of lipids from fermentation by *Rhodococcus*. Previous studies have shown that the fermentation and digestion of complex substrates, such as cellulose and other polysaccharides, mainly takes place in the cecum of chickens because the microbes are more abundant there and the fodder lasts longer at this site (Sergeant et al., 2014; AL-Darkazali et al., 2017), whereas the fermentation of complex carbohydrates in the small intestine is limited. However, our study revealed that these apparently indigestible carbohydrates can be degraded by some microbes in the small intestine, which may have a positive impact on the growth and production performance of broiler chickens. After all, the small intestine is the main site for the digestion and absorption of nutrients. In addition, the nonstarch polysaccharides in the feed components are prone to form mixed colloids with lignin and resistant starch, which increases the viscosity of the intestinal chyme and thus reduces the total digestibility of nutrients in chickens (Lovegrove et al., 2017). Therefore, if we could identify the microbes that can degrade these colloidal substances effectively in the small intestine and then improve their relative abundance, the endogenous digestive enzymes may show better contact with the fodder particles, thereby improving the digestibility.

It has been reported that certain ET or major microbial taxa are associated to some extent with human disease states (Ou et al., 2013; de Moraes et al., 2017), but there are relatively few related studies on animals. Although some studies have shown that the gut microbiota plays a role in the regulation of animal host phenotypes, such as fat deposition (Wen et al., 2019), these traits are also affected by factors such as the host's own heredity and nutritional environment. Therefore, more scientific evaluation of the role of the microbiota in this process is needed. In terms of phenotypes, we observed that the ET2 group had the maximum values of TG, SFT, and AFW but did not show the highest body weight, indicating that fat deposition in the ET2 group was higher than in the other 2 ET groups. An explanation for this may be that the dominant microorganism in the ET2 population, *Rhodococcus*, which first generates tridecanoic acid and glycerol 1-myristate as LCFA, and then, these LCFA are absorbed and used by broilers themselves as nutrients, which can promote the synthesis of TG and further deposit body fat in broilers. Gut microbes can degrade some plant polysaccharides that cannot be used by the host itself, such as pectin, cellulose, hemicellulose, and resistant starch, and produce monosaccharides or short-chain fatty acids that are beneficial for the host to absorb nutrients (Tremaroli and Bäckhed, 2012). In this study, this biological process occurred during the combined degradation of plant lignocellulose by *Ochrobactrum* and *Rhodococcus*. Furthermore, monosaccharides and short-chain fatty acids can promote the synthesis of liver fat and the conversion of TG into adipose tissue (Bäckhed et al., 2004).

CONCLUSIONS

In conclusion, we performed ET identification of the duodenal microbiome community of 206 broiler chickens, detected the metabolic profile of the representatives of each ET, and analyzed the complete microbiome. Similar to mammals, we identified 3 ET in the broiler population, and significant differences in the microflora structure and function were observed among ET. We found that several simple sugars (e.g., cellobiose, mannose, and allose) might be associated with the combined degradation of lignocellulose by bacterial genera *Ochrobactrum* and *Rhodococcus*. In addition, we found that the abundance of tridecanoic acid and glycerol 1-myristate was consistent with the abundance of the triacylglycerol-producing bacterial genus *Rhodococcus*, which indicates the phenotype of lipid-generation characteristic of this genus. Collectively, these findings extend the applicability of the ET concept in poultry and provide new insights into the role of gut microbes in food digestion and absorption, which contribute to our understanding of the interactions between gut microbes and broilers.

ACKNOWLEDGMENTS

The present study was supported by Programs for Changjiang Scholars and Innovative Research in University (IRT_15R62), China Agriculture Research System (CARS-40) and Chinese Universities Scientific Fund (2019TC212).

SUPPLEMENTARY DATA

Supplementary data associated with this article can be found in the online version at https://doi.org/10.1016/j.psj.2019.10.078.

REFERENCES

AL-Darkazali, H., V. Meevootisom, D. Isarangkul, and S. Wiyakrutta. 2017. Gene expression and molecular characterization of a xylanase from chicken cecum metagenome. Int. J. Microbiol. 2017:12.

Alvarez, H. M., R. Kalscheuer, and A. Steinbuchel. 2000. Accumulation and mobilization of storage lipids by Rhodococcus opacus PD630 and Rhodococcus ruber NCIMB 40126. Appl. Microbiol. Biotechnol. 54:218–223.

Arumugam, M., J. Raes, E. Pelletier, D. Le Paslier, T. Yamada, D. R. Mende, G. R. Fernandes, J. Tap, T. Bruls, J. Batto, M. Bertalan, N. Borruel, F. Casellas, L. Fernandez, L. Gautier, T. Hansen, M. Hattori, T. Hayashi, M. Kleerebezem, K. Kurokawa, M. Leclerc, F. Levenez, C. Manichanh, H. B. Nielsen, T. Nielsen, N. Pons, J. Poulain, J. Qin, T. Sicheritz-Ponten, S. Tims, D. Torrents, E. Ugarte, E. G. Zoetendal, J. Wang, F. Guarner, O. Pedersen, W. M. de Vos, S. Brunak, J. Doré, M. Antolín, F. Artiguenave, H. M. Blottiere, M. Almeida, C. Brechot, C. Cara, C. Chervaux, A. Cultrone, C. Delorme, G. Denariaz, R. Dervyn, K. U. Foerstner, C. Friss, M. van de Guchte, E. Guedon, F. Haimet, W. Huber, J. van Hylckama-Vlieg, A. Jamet, C. Juste, G. Kaci, J. Knol, O. Lakhdari, S. Layec, K. Le Roux, E. Maguin, A. Mérieux, R. Melo Minardi, C. M'Rini, J. Muller, R. Oozeer, J. Parkhill, P. Renault, M. Rescigno, N. Sanchez, S. Sunagawa, A. Torrejon, K. Turner, G. Vandemeulebrouck, E. Varela, Y. Winogradsky, G. Zeller, J. Weissenbach, S. D. Ehrlich, and P. Bork. 2011. Enterotypes of the human gut microbiome. Nature 473:174–180.

Bäckhed, F., H. Ding, T. Wang, L. V. Hooper, G. Y. Koh, A. Nagy, C. F. Semenkovich, and J. I. Gordon. 2004. The gut microbiota as an environmental factor that regulates fat storage. Proc. Natl. Acad. Sci. U. S. A. 101:15718–15723.

Bang, C., T. Dagan, P. Deines, N. Dubilier, W. J. Duschl, S. Fraune, U. Hentschel, H. Hirt, N. Hülter, T. Lachnit, D. Picazo, L. Pita, C. Pogoreutz, N. Rädecker, M. M. Saad, R. A. Schmitz, H. Schulenburg, C. R. Voolstra, N. Weiland-Bräuer, M. Ziegler, and T. C. G. Bosch. 2018. Metaorganisms in extreme environments: Do microbes play a role in organismal adaptation? Zoology 127:1–19.

Cervantes-Barragan, L., J. N. Chai, M. D. Tianero, B. Di Luccia, P. P. Ahern, J. Merriman, V. S. Cortez, M. G. Caparon, M. S. Donia, S. Gilfillan, M. Cella, J. I. Gordon, C. Hsieh, and M. Colonna. 2017. Lactobacillus reuteri induces gut intraepithelial CD4(+)CD8αα(+) T cells. Science 357:806–810.

Cho, I., S. Yamanishi, L. Cox, B. A. Methé, J. Zavadil, K. Li, Z. Gao, D. Mahana, K. Raju, I. Teitler, H. Li, A. V. Alekseyenko, and M. J. Blaser. 2012. Antibiotics in early life alter the murine colonic microbiome and adiposity. Nature 488:621.

Choi, J. H., G. B. Kim, and C. J. Cha. 2014. Spatial heterogeneity and stability of bacterial community in the gastrointestinal tracts of broiler chickens. Poult. Sci. 93:1942–1950.

Cocking, E. C. 2003. Endophytic colonization of plant roots by nitrogen-fixing bacteria. Plant and Soil 252:169–175.

Costea, P. I., F. Hildebrand, M. Arumugam, F. Bäckhed, M. J. Blaser, F. D. Bushman, W. M. de Vos, S. D. Ehrlich, C. M. Fraser, M. Hattori, C. Huttenhower, I. B. Jeffery, D. Knights, J. D. Lewis, R. E. Ley, H. Ochman, P. W. O Toole, C. Quince, D. A. Relman, F. Shanahan, S. Sunagawa, J. Wang, G. M. Weinstock, G. D. Wu, G. Zeller, L. Zhao, J. Raes, R. Knight, and P. Bork. 2018. Enterotypes in the landscape of gut microbial community composition. Nat. Microbiol. 3:8–16.

Davail, S., K. Ricaud, M. Even, F. Lavigne, and J. Arroyo. 2018. Evolution of intestinal microbiota and body compartments during spontaneous hyperphagia in the Greylag goose. Poult. Sci. 98:1390–1402.

De Filippo, C., D. Cavalieri, M. Di Paola, M. Ramazzotti, J. B. Poullet, S. Massart, S. Collini, G. Pieraccini, and P. Lionetti. 2010. Impact of diet in shaping gut microbiota revealed by a comparative study in children from Europe and rural Africa. Proc. Natl. Acad. Sci. U. S. A. 107:14691–14696.

de Gonzalo, G., D. I. Colpa, M. H. M. Habib, and M. W. Fraaije. 2016. Bacterial enzymes involved in lignin degradation. J. Biotechnol. 236:110–119.

de Moraes, A. C. F., G. R. Fernandes, I. T. Da Silva, B. Almeida-Pititto, E. P. Gomes, A. D. C. Pereira, and S. R. G. Ferreira. 2017. Enterotype may drive the Dietary-Associated cardiometabolic risk factors. Front. Cell. Infect. Microbiol. 7:47.

Falony, G., M. Joossens, S. Vieira-Silva, J. Wang, Y. Darzi, K. Faust, A. Kurilshikov, M. J. Bonder, M. Valles-Colomer, D. Vandeputte, R. Y. Tito, S. Chaffron, L. Rymenans, C. Verspecht, L. De Sutter, G. Lima-Mendez, K. D. Hoe, K. Jonckheere, D. Homola, R. Garcia, E. F. Tigchelaar, L. Eeckhaudt, J. Fu, L. Henckaerts, A. Zhernakova, C. Wijmenga, and J. Raes. 2016. Population-level analysis of gut microbiome variation. Science 352:560–564.

Fiehn, O. 2002. Metabolomics – the link between genotypes and phenotypes. Plant Mol. Biol. 48:155–171.

Franche, C., K. Lindström, and C. Elmerich. 2009. Nitrogen-fixing bacteria associated with leguminous and non-leguminous plants. Plant Soil 321:35–59.

Franzosa, E. A., A. Sirota-Madi, J. Avila-Pacheco, N. Fornelos, H. J. Haiser, S. Reinker, T. Vatanen, A. B. Hall, H. Mallick, L. J. McIver, J. S. Sauk, R. G. Wilson, B. W. Stevens, J. M. Scott, K. Pierce, A. A. Deik, K. Bullock, F. Imhann, J. A. Porter, A. Zhernakova, J. Fu, R. K. Weersma, C. Wijmenga, C. B. Clish, H. Vlamakis, C. Huttenhower, and R. J. Xavier. 2019. Gut microbiome structure and metabolic activity in inflammatory bowel disease. Nat. Microbiol. 4:293–305.

Hildebrand, F., T. L. Nguyen, B. Brinkman, R. G. Yunta, B. Cauwe, P. Vandenabeele, A. Liston, and J. Raes. 2013. Inflammation-associated enterotypes, host genotype, cage and inter-individual effects drive gut microbiota variation in common laboratory mice. Genome Biol. 14:R4.

Huse, S. M., Y. Ye, Y. Zhou, and A. A. Fodor. 2012. A core human microbiome as viewed through 16S rRNA sequence clusters. Plos One 7:e34242.

Imran, A., F. Y. Hafeez, A. Fruhling, P. Schumann, K. A. Malik, and E. Stackebrandt. 2010. Ochrobactrum ciceri sp. Nov., isolated from nodules of Cicer arietinum. Int. J. Syst. Evol. Microbiol. 60:1548–1553.

Jansson, J. K., and E. S. Baker. 2016. A multi-omic future for microbiome studies. Nat. Microbiol. 1:16049.

Kaakoush, N. O., N. Sodhi, J. W. Chenu, J. M. Cox, S. M. Riordan, and H. M. Mitchell. 2014. The interplay between Campylobacter and Helicobacter species and other gastrointestinal microbiota of commercial broiler chickens. Gut Pathog. 6:18.

Kessner, D., D. Agus, M. Chambers, P. Mallick, and R. Burke. 2008. ProteoWizard: Open source software for rapid proteomics tools development. Bioinformatics 24:2534–2536.

Koren, O., D. Knights, A. Gonzalez, L. Waldron, N. Segata, R. Knight, C. Huttenhower, and R. E. Ley. 2013. A guide to enterotypes across the human body: Meta-analysis of microbial community structures in human microbiome datasets. Plos Comput. Biol. 9:e1002863.

Kosa, M., and A. J. Ragauskas. 2012. Bioconversion of lignin model compounds with oleaginous Rhodococci. Appl. Microbiol. Biotechnol. 93:891–900.

Li, J., J. E. Powell, J. Guo, J. D. Evans, J. Wu, P. Williams, Q. Lin, N. A. Moran, and Z. Zhang. 2015. Two gut community enterotypes recur in diverse bumblebee species. Curr. Biol. 25:R652–R653.

Liang, C., H. Tseng, H. Chen, W. Wang, C. Chiu, J. Chang, K. Lu, S. Weng, T. Chang, C. Chang, C. Weng, H. Wang, and

H. Huang. 2017. Diversity and enterotype in gut bacterial community of adults in Taiwan. BMC Genomics 18:932.
Liu, Z. H., S. Xie, F. Lin, M. Jin, and J. S. Yuan. 2018. Combinatorial pretreatment and fermentation optimization enabled a record yield on lignin bioconversion. Biotechnol. Biofuels 11:21.
Lovegrove, A., C. H. Edwards, I. De Noni, H. Patel, S. N. El, T. Grassby, C. Zielke, M. Ulmius, L. Nilsson, P. J. Butterworth, P. R. Ellis, and P. R. Shewry. 2017. Role of polysaccharides in food, digestion, and health. Crit. Rev. Food Sci. Nutr. 57:237–253.
MacEachran, D. P., M. E. Prophete, and A. J. Sinskey. 2010. The rhodococcus opacus PD630 Heparin-Binding hemagglutinin homolog TadA mediates lipid body formation. Appl. Environ. Microbiol. 76:7217–7225.
Mach, N., M. Berri, J. Estellé, F. Levenez, G. Lemonnier, C. Denis, J. Leplat, C. Chevaleyre, Y. Billon, J. Doré, C. Rogel-Gaillard, and P. Lepage. 2015. Early-life establishment of the swine gut microbiome and impact on host phenotypes. Environ. Microbiol. Rep. 7:554–569.
Moeller, A. H., P. H. Degnan, A. E. Pusey, M. L. Wilson, B. H. Hahn, and H. Ochman. 2012. Chimpanzees and humans harbour compositionally similar gut enterotypes. Nat. Commun. 3:1179.
Ndeh, D., A. Rogowski, A. Cartmell, A. S. Luis, A. Baslé, J. Gray, I. Venditto, J. Briggs, X. Zhang, A. Labourel, N. Terrapon, F. Buffetto, S. Nepogodiev, Y. Xiao, R. A. Field, Y. Zhu, M. A. O Neill, B. R. Urbanowicz, W. S. York, G. J. Davies, D. W. Abbott, M. Ralet, E. C. Martens, B. Henrissat, and H. J. Gilbert. 2017. Complex pectin metabolism by gut bacteria reveals novel catalytic functions. Nature 544:65.
Ngom, A., Y. Nakagawa, H. Sawada, J. Tsukahara, S. Wakabayashi, T. Uchiumi, A. Nuntagij, S. Kotepong, A. Suzuki, S. Higashi, and M. Abe. 2004. A novel symbiotic nitrogen-fixing member of the Ochrobactrum clade isolated from root nodules of Acacia mangium. J. Gen. Appl. Microbiol. 50:17.
Ou, J., F. Carbonero, E. G. Zoetendal, J. P. DeLany, M. Wang, K. Newton, H. R. Gaskins, and S. J. D. O'Keefe. 2013. Diet, microbiota, and microbial metabolites in colon cancer risk in rural Africans and African Americans. Am. J. Clin. Nutr. 98:111–120.
Plomion, C., G. Leprovost, and A. Stokes. 2001. Wood formation in trees. Plant Physiol. 127:1513–1523.
Qin, J., Y. Li, Z. Cai, S. Li, J. Zhu, F. Zhang, S. Liang, W. Zhang, Y. Guan, D. Shen, Y. Peng, D. Zhang, Z. Jie, W. Wu, Y. Qin, W. Xue, J. Li, L. Han, D. Lu, P. Wu, Y. Dai, X. Sun, Z. Li, A. Tang, S. Zhong, X. Li, W. Chen, R. Xu, M. Wang, Q. Feng, M. Gong, J. Yu, Y. Zhang, M. Zhang, T. Hansen, G. Sanchez, J. Raes, G. Falony, S. Okuda, M. Almeida, E. LeChatelier, P. Renault, N. Pons, J. Batto, Z. Zhang, H. Chen, R. Yang, W. Zheng, S. Li, H. Yang, J. Wang, S. D. Ehrlich, R. Nielsen, O. Pedersen, K. Kristiansen, and J. Wang. 2012. A metagenome-wide association study of gut microbiota in type 2 diabetes. Nature 490:55–60.
Semova, I., J. D. Carten, J. Stombaugh, L. C. Mackey, R. Knight, S. A. Farber, and J. F. Rawls. 2012. Microbiota regulate intestinal absorption and metabolism of fatty acids in the zebrafish. Cell Host & Microbe 12:210–277.
Sergeant, M. J., C. Constantinidou, T. A. Cogan, M. R. Bedford, C. W. Penn, and M. J. Pallen. 2014. Extensive microbial and functional diversity within the chicken cecal microbiome. Plos One 9:e91941.
Shaffer, M., A. J. S. Armstrong, V. V. Phelan, N. Reisdorph, and C. A. Lozupone. 2017. Microbiome and metabolome data integration provides insight into health and disease. Transl. Res. 189:51–64.
Stanley, D., S. E. Denman, R. J. Hughes, M. S. Geier, T. M. Crowley, H. Chen, V. R. Haring, and R. J. Moore. 2012. Intestinal microbiota associated with differential feed conversion efficiency in chickens. Appl. Microbiol. Biotechnol. 96:1361–1369.
Tautenhahn, R., G. J. Patti, D. Rinehart, and G. Siuzdak. 2012. XCMS Online: a web-based platform to process untargeted metabolomic data. Anal. Chem. 84:5035–5039.
Tremaroli, V., and F. Bäckhed. 2012. Functional interactions between the gut microbiota and host metabolism. Nature 489:242.
Ursell, L. K., J. L. Metcalf, L. W. Parfrey, and R. Knight. 2012. Defining the human microbiome. Nutr. Rev. 70:S38–S44.
Wang, J., M. Linnenbrink, S. Künzel, R. Fernandes, M. Nadeau, P. Rosenstiel, and J. F. Baines. 2014. Dietary history contributes to enterotype-like clustering and functional metagenomic content in the intestinal microbiome of wild mice. Proc. Natl. Acad. Sci. U. S. A. 111:E2703–E2710.
Wen, C., W. Yan, C. Sun, C. Ji, Q. Zhou, D. Zhang, J. Zheng, and N. Yang. 2019. The gut microbiota is largely independent of host genetics in regulating fat deposition in chickens. ISME J. 13:1422–1436.
Wilhelm, R. C., R. Singh, L. D. Eltis, and W. W. Mohn. 2019. Bacterial contributions to delignification and lignocellulose degradation in forest soils with metagenomic and quantitative stable isotope probing. ISME J. 13:413–429.
Woo, S. G., L. N. Ten, J. Park, and M. Lee. 2011. Ochrobactrum daejeonense sp. Nov., A nitrate-reducing bacterium isolated from sludge of a leachate treatment plant. Int. J. Syst. Evol. Microbiol. 61:2690–2696.
Wu, G. D., J. Chen, C. Hoffmann, K. Bittinger, Y. Y. Chen, S. A. Keilbaugh, M. Bewtra, D. Knights, W. A. Walters, R. Knight, R. Sinha, E. Gilroy, K. Gupta, R. Baldassano, L. Nessel, H. Li, F. D. Bushman, and J. D. Lewis. 2011. Linking Long-Term dietary patterns with gut microbial enterotypes. Science 334:105–108.
Xiao, Y., Y. Xiang, W. Zhou, J. Chen, K. Li, and H. Yang. 2017. Microbial community mapping in intestinal tract of broiler chicken. Poult. Sci. 96:1387–1393.
Yan, W., C. Sun, J. Zheng, C. WEN, C. Ji, D. Zhang, Y. Chen, Z. Hou, and N. Yang. 2019. Efficacy of fecal sampling as a gut proxy in the study of chicken gut microbiota. Front. Microbio. 10:2126.
Yatsunenko, T., F. E. Rey, M. J. Manary, I. Trehan, M. G. Dominguez-Bello, M. Contreras, M. Magris, G. Hidalgo, R. N. Baldassano, A. P. Anokhin, A. C. Heath, B. Warner, J. Reeder, J. Kuczynski, J. G. Caporaso, C. A. Lozupone, C. Lauber, J. C. Clemente, D. Knights, R. Knight, and J. I. Gordon. 2012. Human gut microbiome viewed across age and geography. Nature 486:222–227.
Zhao, Y., J. Wu, J. V. Li, N. Zhou, H. Tang, and Y. Wang. 2013. Gut microbiota composition modifies fecal metabolic profiles in mice. J. Proteome Res. 12:2987–2999.
Zhou, Y., K. A. Mihindukulasuriya, H. Gao, P. S. La Rosa, K. M. Wylie, J. C. Martin, K. Kota, W. D. Shannon, M. Mitreva, E. Sodergren, and G. M. Weinstock. 2014. Exploration of bacterial community classes in major human habitats. Genome Biol. 15:R66.
Zierer, J., M. A. Jackson, G. Kastenmüller, M. Mangino, T. Long, A. Telenti, R. P. Mohney, K. S. Small, J. T. Bell, C. J. Steves, A. M. Valdes, T. D. Spector, and C. Menni. 2018. The fecal metabolome as a functional readout of the gut microbiome. Nat. Genet. 50:790–795.
Zupancic, M. L., B. L. Cantarel, Z. Liu, E. F. Drabek, K. A. Ryan, S. Cirimotich, C. Jones, R. Knight, W. A. Walters, D. Knights, E. F. Mongodin, R. B. Horenstein, B. D. Mitchell, N. Steinle, S. Snitker, A. R. Shuldiner, and C. M. Fraser. 2012. Analysis of the gut microbiota in the old order amish and its relation to the metabolic syndrome. Plos One 7:e43052.
Zurdo-Pineiro, J. L., R. Rivas, M. E. Trujillo, N. Vizcaino, J. A. Carrasco, M. Chamber, A. Palomares, P. F. Mateos, E. Martinez-Molina, and E. Velazquez. 2007. Ochrobactrum cytisi sp. Nov., isolated from nodules of Cytisus scoparius in Spain. Int. J. Syst. Evol. Microbiol. 57:784–788.